Blockade of activin type II receptors with a dual anti-ActRIIA/IIB antibody is critical to promote maximal skeletal muscle hypertrophy

Frederic Morvan[a], Jean-Michel Rondeau[b], Chao Zou[b], Giulia Minetti[a], Clemens Scheufler[b], Meike Scharenberg[c], Carsten Jacobi[a], Pascale Brebbia[a], Veronique Ritter[a], Gauthier Toussaint[a], Claudia Koelbing[a], Xavier Leber[c], Alain Schilb[a], Florian Witte[d], Sylvie Lehmann[b], Elke Koch[b], Sabine Geisse[c], David J. Glass[e], and Estelle Lach-Trifilieff[a,1]

[a]MusculoSkeletal Diseases, Novartis Institutes for Biomedical Research, 4002 Basel, Switzerland; [b]Chemical Biology and Therapeutics, Structural Biophysics Group, Novartis Institutes for Biomedical Research, 4002 Basel, Switzerland; [c]Novartis Biologics Center, Novartis Institutes for Biomedical Research, 4002 Basel, Switzerland; [d]MorphoSys AG, 82152 Martinsried/Planegg, Germany; and [e]Chemical Biology and Therapeutics, Novartis Institutes for Biomedical Research, Cambridge, MA 02139

Edited by Se-Jin Lee, Johns Hopkins University, Baltimore, MD, and approved October 11, 2017 (received for review May 15, 2017)

The TGF-β family ligands myostatin, GDF11, and activins are negative regulators of skeletal muscle mass, which have been reported to primarily signal via the ActRIIB receptor on skeletal muscle and thereby induce muscle wasting described as cachexia. Use of a soluble ActRIIB-Fc "trap," to block myostatin pathway signaling in normal or cachectic mice leads to hypertrophy or prevention of muscle loss, perhaps suggesting that the ActRIIB receptor is primarily responsible for muscle growth regulation. Genetic evidence demonstrates however that both ActRIIB- and ActRIIA-deficient mice display a hypertrophic phenotype. Here, we describe the mode of action of bimagrumab (BYM338), as a human dual-specific anti-ActRIIA/ActRIIB antibody, at the molecular and cellular levels. As shown by X-ray analysis, bimagrumab binds to both ActRIIA and ActRIIB ligand binding domains in a competitive manner at the critical myostatin/activin binding site, hence preventing signal transduction through either ActRII. Myostatin and the activins are capable of binding to both ActRIIA and ActRIIB, with different affinities. However, blockade of either single receptor through the use of specific anti-ActRIIA or anti-ActRIIB antibodies achieves only a partial signaling blockade upon myostatin or activin A stimulation, and this leads to only a small increase in muscle mass. Complete neutralization and maximal anabolic response are achieved only by simultaneous blockade of both receptors. These findings demonstrate the importance of ActRIIA in addition to ActRIIB in mediating myostatin and activin signaling and highlight the need for blocking both receptors to achieve a strong functional benefit.

activin | myostatin | ActRII | dual antibody | hypertrophy

Skeletal muscle wasting occurs in a variety of pathophysiological settings, including sepsis, renal failure, diabetes, chronic obstructive pulmonary disease, and cancer (1). Muscle atrophy also occurs from casting, immobilization, or prolonged bed rest (2), and in the age-related loss of skeletal muscle known as sarcopenia, which is a component of the larger concept of frailty and weakness often observed in elderly individuals (3, 4). Several negative regulators of muscle mass have been reported to act through the activin receptor type IIB (ActRIIB) (5, 6). The best characterized ligands are myostatin [also known as growth and differentiation factor 8 (GDF8)] (7–9) and activin A (10–13), while there is some uncertainty with regard to the contribution of GDF11 (13–15) at regulating muscle mass and function, although it has been demonstrated that administration of GDF11 inhibits regeneration in a dose-responsive fashion (16, 17). Indeed, all those ligands are able to inhibit muscle differentiation and to induce muscle fiber atrophy. Recent work examining the relative contribution of various ligands, activin A, activin B, beyond myostatin, unveiled a strong synergistic response upon blockade of both activin and myostatin (18, 19), with some cross-species difference between mice and primates (18).

Myostatin and activin A bind to and signal through either ActRIIA or ActRIIB on the cell membrane, with ActRIIB initially identified as myostatin's prime receptor (20).

Multiple myostatin pathway inhibitors, all aiming at ligand(s) neutralization, have been generated with the therapeutic aim of stimulating muscle growth or preventing muscle loss in settings of human muscle disease. These pharmacological candidates include neutralizing antibodies to myostatin (21–23), a modified myostatin propeptide which blocks myostatin (24), as well as broader agents, such as a soluble ActRIIB-Fc "receptor trap" (11, 25–27), neutralizing any ligand capable of binding ActRIIB, including ligands which have affinity for other TGF-β receptors (13), and an anti-ActRII receptor antibody, bimagrumab, which was shown to prevent myostatin and activin A signaling (28). All of these approaches have been shown to increase postnatal muscle growth in mice, albeit to different degrees—pure myostatin inhibition being

Significance

We recently reported that activin type II receptors (ActRIIs) blockade using bimagrumab could positively impact muscle wasting in mice and humans. However, the specific role of each individual ActRII at regulating adult muscle mass had not been clarified. Here, we highlight the importance of concomitant neutralization of both ActRIIs in controlling muscle mass. Through comparison with single specificity antibodies, we uncover unique features related to bimagrumab and its neutralizing interactions with both ActRIIA and ActRIIB at the structural and cellular levels and in vivo in adult mice. The need for simultaneous engagement and neutralization of both ActRIIs to generate a strong skeletal muscle response confers unique therapeutic potential to bimagrumab, in the context of muscle wasting conditions.

Author contributions: F.M., J.-M.R., C.Z., G.M., M.S., C.J., S.G., D.J.G., and E.L.-T. designed research; J.-M.R., C.Z., C.S., P.B., V.R., G.T., C.K., X.L., A.S., F.W., S.L., E.K., and S.G. performed research; C.S., S.L., E.K., and S.G. contributed new reagents/analytic tools; F.M., J.-M.R., C.Z., G.M., M.S., C.J., S.G., D.J.G., and E.L.-T. analyzed data; and F.M., J.-M.R., G.M., D.J.G., and E.L.-T. wrote the paper.

Conflict of interest statement: All authors but F.W. are employees of Novartis Pharma AG (F.M., C.Z., C.S., J.-M.R., C.J., A.S., P.B., V.R., G.T., M.K., X.L., S.L., E.K., G.M., C.K., S.G., D.J.G., E.L.-T.), and some are also shareholders of Novartis. F.W. was an employee of MorphoSys AG at the time of contribution.

This article is a PNAS Direct Submission.

Data deposition: Coordinates and structure factors for the bimagrumab Fab, the bimagrumab Fv complex with the ActRIIA-LBD, and with ActRIIB-LBD (cubic and orthorhombic crystal forms) are available from the Protein Data Bank under accession codes 5NHW, 5NH3, 5NHR, and 5NGV, respectively.

[1]To whom correspondence should be addressed. Email: estelle.trifilieff@novartis.com.

This article contains supporting information online at www.pnas.org/lookup/suppl/doi:10.1073/pnas.1707925114/-/DCSupplemental.

less effective than the broader approaches when administered postnatally. Administration of soluble ActRIIB or of anti-ActRII antibody led to muscle hypertrophy both in naive and in myostatin knockout mice, confirming that other activin type II receptor ligands besides myostatin contribute to the inhibition of muscle growth (11, 28). Both agents also prevented muscle wasting in several disease models, ranging from glucocorticoid-induced atrophy (28) to cancer cachexia (26, 29), as indeed myostatin and activin A had been reported to induce muscle wasting and cachexia (5, 6, 30). The development of an anti-ActRII neutralizing antibody represents a potential therapeutic entry for the treatment of multiple conditions associated with muscle wasting, by significantly reducing the activity of myostatin, activin A, and GDF11. While there has been a lot of focus on ActRIIB in particular, we present here evidence for the need to neutralize both ActRIIA and ActRIIB, as opposed to selective inhibition of either of the two receptors, ActRIIA or ActRIIB, for an anabolic response in adult rodents.

Results

Bimagrumab Binds to both ActRIIA and ActRIIB Ligand Binding Domains. The crystal structures of the Bimagrumab Fv fragment in complex with the human ActRIIA and ActRIIB ligand binding domains (LBDs) were determined at 2.35-Å and 2.00-Å resolution, respectively (Fig. 1 and *SI Appendix*, Table S1). The human ActRIIA and ActRIIB LBDs share 55% amino acid sequence identity (*SI Appendix*, Fig. S1) and the same "three-finger toxin fold" (31), a seven-stranded antiparallel β-sheet stabilized by five disulfide bridges. Bimagrumab binds to the concave face of the LBDs (Fig. 1 *A* and *B*), with excellent electrostatic and shape complementarity (*SI Appendix*, Fig. S2 and Table S2). The epitopes for ActRIIA and ActRIIB LBD involve residues spread over many distinct elements of secondary structure, the β4–β5 loop playing, however, a conserved central role for both receptors (Fig. 2). The epitopes include many acidic residues and several exposed aromatic residues (Fig. 2 and *SI Appendix*, Table S2). A structural overlay of the two Fv complexes shows that the antibody binds the two LBDs in the same way, despite the relatively low overall conservation (65%) of all epitope residues (Fig. 1*D*). The affinity of the bimagrumab Fab for ActRIIA (K_d = 973 pM) is >50-fold lower in comparison with ActRIIB (K_d = 16 pM) and in line with a prior report (28). An in-depth inspection of the binding interface suggests that Trp78, Asp80, Phe82, Asn83, Glu52, and Phe101 are particularly important epitope residues of the ActRIIB LBD. Two of these residues are different in ActRIIA: Glu52 is an aspartic acid and Phe82, an isoleucine. While these differences may appear conservative, they result in the loss of a strong salt bridge between Glu52 and Arg98 of H-CDR3, and in the loss of multiple aromatic–aromatic interactions between Phe82 and Trp101 of H-CDR3, Phe93 and Tyr98 of L-CDR3, and Tyr32 of L-CDR1. Interestingly, a further consequence of the Glu52Asp difference is a change in conformation of the corresponding epitope loop (β2–β3), which moves away from the antibody and retains flexibility in the complex, as judged from its relatively higher temperature factors (*SI Appendix*, Fig. S3). The β5–β6 loop, which contributes few binding interactions in the ActRIIB complex, is also shifted away from the antibody in the ActRIIA complex, albeit to a lesser extent. Taken together, and in comparison with the ActRIIB complex, the shift of these two loops leads to a significant decrease in the number of LBD residues located at the antibody interface (20 instead of 29) and in the amount of buried solvent-accessible surface (1,547 Å^2 instead 2,047 Å^2). Therefore, the reduced binding affinity of bimagrumab to ActRIIA compared with ActRIIB can be mainly ascribed to two mutations affecting important epitope residues (Glu52 to Asp and Phe82 to Ile), which lead to a reduction in the size of the binding interface and in the total number of intermolecular interactions.

We have also determined the structure of the bimagrumab Fab in the unliganded state at 1.78-Å resolution. A structural overlay of the antibody V_H/V_L domain in the free and antigen-bound states does not reveal any large conformational changes affecting the paratope and shows that bimagrumab binds the ActRII LBDs by a mainly rigid lock-and-key-fit mechanism (*SI Appendix*, Fig. S4). The very high, picomolar binding affinity of bimagrumab toward the ActRIIB LBD results from an unusually good shape complementarity, combined with strong electrostatic and hydrophobic interactions involving all six CDRs, and a lock-and-key-fit mechanism of association.

The surface of the ActRII LBD involved in ligand binding has been revealed by crystallographic analyses of the BMP-2 (32) and BMP-7 (33) complexes with the mouse ActRIIA LBD and the human BMP-2 (34), and activin A (35, 36) complexes with mouse or rat ActRIIB LBD. As examplified in Fig. 1*C* with the activin complex, the natural ligand binds to the concave side of the ActRII LBD, and the overlap between the ligand and the antibody binding surfaces is therefore extensive (Fig. 1 *E* and *F*). Hence, bimagrumab blocks a functional epitope at the ligand binding surface on the ActRIIA and ActRIIB LBD and therefore directly competes with ligand binding to these receptors, thus preventing signaling, as described below.

Cellular Role of ActRIIA and ActRIIB in Response to Myostatin and Activin A. We generated ActRIIA-specific and ActRIIB-specific antibodies, which bound, respectively, with 488-pM affinity to

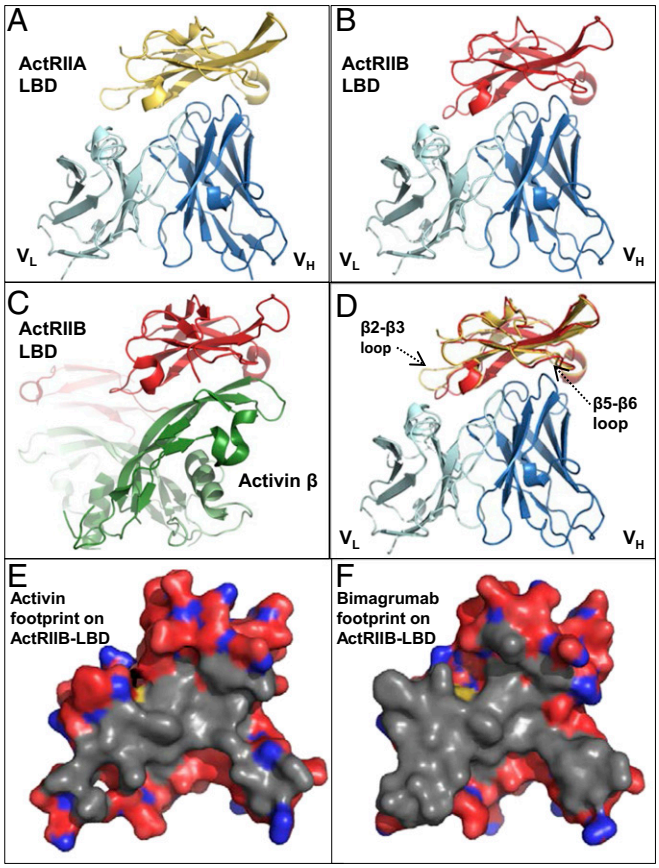

Fig. 1. Binding modalities of bimagrumab to ActRIIA and ActRIIB. Crystal structures of the bimagrumab Fv (light/dark blue ribbon) complex with (*A*) human ActRIIA LBD (gold ribbon) or (*B*) human ActRIIB LBD (red ribbon), shown in the same orientation. (*C*) Crystal structure of the mouse ActRIIB LBD complex with human activin-β (PDB entry 1S4Y) (35), shown in the same orientation as in *A*, *B*, and *D*. (*D*) Overlay of the ActRIIA Fv complex (gold ribbon) and ActRIIB Fv complex (red ribbon). (*E*) Footprint of activin (gray surface, calculated from PDB entry 1S4Y) and (*F*) bimagrumab on the ActRIIB LBD. Note the extensive overlap between the two binding surfaces.

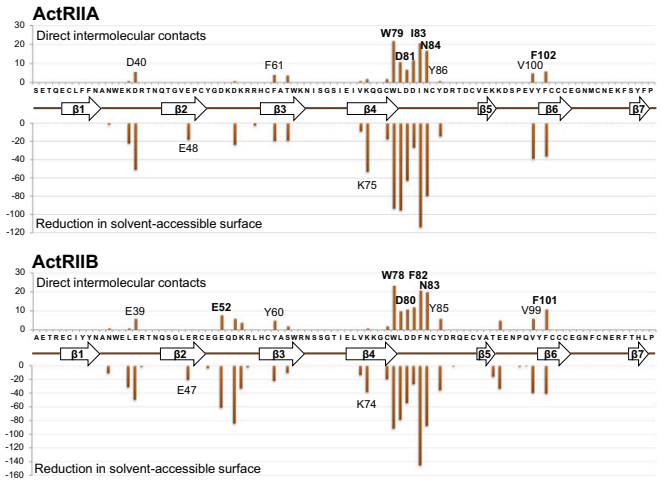

Fig. 2. ActRIIA (*Upper*) and ActRIIB (*Lower*) epitope recognized by bimagrumab. The *Upper* part of each panel shows the number of direct intermolecular contacts between nonhydrogen atoms within a 4.0-Å distance; *Lower* part shows the reduction in solvent-accessible surface upon complex formation. The amino acid sequence of the respective ActRII LBD is displayed on the horizontal axis, together with a schematic representation of the secondary structure elements (arrows, β-strands; thick lines, connecting loops).

ActRIIA for antibody CSJ089 and with 64-pM affinity to ActRIIB for antibody CQI876 (each antibody demonstrated no detectable binding to the other activin type II receptor). Bimagrumab and the other antibodies described here, displayed no cross-reactivity to a panel of antigens, including Alk4, Alk5, TGF-βRII, TGF-βRIIB, BMPRII, and MISRII, up to concentrations 1,000-fold above the affinity for their target antigen. We thereafter confirmed binding to native cell surface-expressed antigens. Using the specific anti-ActRIIA (CSJ089) and anti-ActRIIB (CQI876) antibodies, very similar staining intensities (*SI Appendix*, Table S3) were detected for both receptors, suggesting similar expression of ActRIIA and ActRIIB in HEK293T/17 cells (Fig. 3*A*). In those cells, we could clearly detect myostatin and activin A induced Smad2/3 signaling through CAGA-Luc reporter gene activity (Fig. 3*B* and *SI Appendix*, Table S4), demonstrating that these receptors were competent to transduce signaling. Using the specific ActRIIA and ActRIIB antibodies and combination thereof as well as the dual antibody bimagrumab, analysis of ActRII receptor usage by myostatin and activin A was investigated. Both myostatin and activin A exhibited binding to ActRIIA and ActRIIB (affinity for ActRIIA, K_d of 701 pM and 5.3 pM and for ActRIIB, K_d of 130 pM and 6.5 pM, for myostatin and activin A, respectively). Upon increasing concentrations of antibodies, only the combination of the anti-ActRIIA and anti-ActRIIB antibodies or the dual-specific antibodies bimagrumab and CDD861 (affinity to ActRIIA, K_d of 134 pM and to ActRIIB, K_d of 62 pM) (Fig. 3*B*) allowed for complete blockade of the myostatin- or activin A-Smad2/3 signaling response. In contrast, treatment with either the anti-ActRIIA or anti-ActRIIB antibody reduced signaling by 30–50% only, clearly demonstrating that myostatin and activin A engage both receptors for triggering their cellular response, and that blockade of a single receptor is not sufficient to completely inhibit signaling, which then operates via the remaining ActRII receptor.

Role of ActRIIA and ActRIIB Neutralization in Hypertrophic in Vivo Response. To assess the relative role of ActRIIA and ActRIIB in mediating muscle hypertrophy, we treated SCID mice weekly for 4 wk with either 6 or 20 mg/kg of the anti-ActRIIA antibody (CSJ089), the anti-ActRIIB antibody (CQI876), the combination of anti-ActRIIA and anti-ActRIIB antibodies, or bimagrumab. Consistent with our previous publication (28), bimagrumab-treated mice exhibited a dose-dependent increase in body weight between 16 and 22% (Fig. 4*A*) compared with sham-treated or control SCID mice, whereas the anti-ActRIIA or anti-ActRIIB Ab-treated mice showed a body weight gain of 10%, whatever the dose administered. These data suggest that this is the maximal response achievable via administration of single-specificity antibodies. Mice receiving the combination of both treatments demonstrated a body mass gain of 22% similar to bimagrumab. The gain in body weight upon bimagrumab intervention correlated with a marked increase of hind-limb muscle mass observed macroscopically at necropsy (Fig. 4*B* and *SI Appendix*, Table S5). The gastrocnemius were increased by 22% and 26%, quadriceps and tibialis anterior by 20–30%, and soleus by 18–38%, with 6 mg/kg/wk and 20 mg/kg/wk treatment, respectively, compared with control SCID mice. Anti-ActRIIA (CSJ089) and anti-ActRIIB (CQI876) antibody-treated mice at both 6 and 20 mg/kg showed an overall muscle hypertrophy of ∼10%, confirming previous observation made on body weight, suggesting target saturation at 6 mg/kg/wk for both anti-ActRIIA and anti-ActRIIB treatments. Compared with bimagrumab, CQI876 has a lower affinity for ActRIIB; however, increasing the dose of CQI876 from 20 mg/kg to 100 mg/kg did not result in a greater magnitude of anabolic response after 2 wk of treatment (Fig. 4*D*), in line with the cellular response to myostatin or activin A achieved upon anti-ActRIIB antibody treatment only. Again, the combination treatment showed an additive response on muscle mass, i.e., muscle hypertrophy demonstrated a dose-dependent increase, and importantly followed the same pattern as the bimagrumab-treated mice compared with control SCID mice.

This pattern of body and muscle weight response already observed 2 wk post-treatment (*SI Appendix*, Fig. S5 *A* and *B*) was reproduced using an anti-ActRIIA antibody with higher affinity, which did not result in a stronger response of the single specific antibody alone. Experiments conducted with another dual antibody CDD861, which exhibited reduced affinity to ActRIIB, better affinity for ActRIIA, and therefore a twofold selectivity

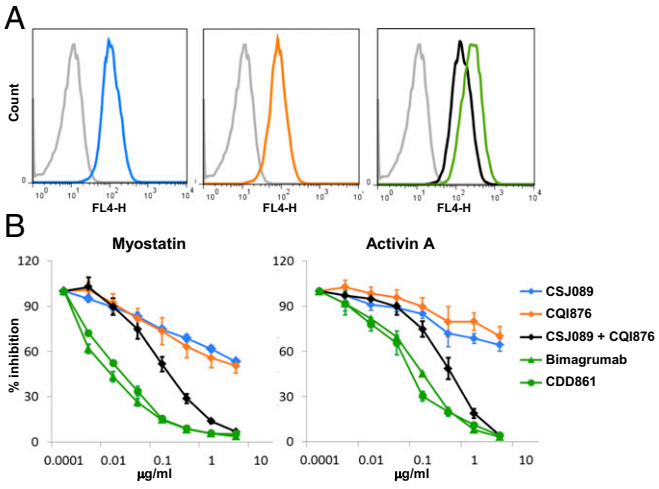

Fig. 3. Cellular responses to ActRIIA and ActRIIB neutralization. (*A*) Binding of anti-ActRIIA (CSJ089, blue), anti-ActRIIB (CQI876, orange), anti-ActRIIA and ActRIIB Abs combination (black), bimagrumab (green), or isotype control Ab (gray) to HEK293T/17 cells. (*B*) Efficacy/potency of antibodies or combination thereof at blocking myostatin or activin A-induced Smad2/3 response. Single-specificity Abs (CSJ089, blue), (CQI876, orange), or combination thereof (CSJ089 and CQI876, black), or bimagrumab (green, triangle) or CDD861 (green, circle) were tested for their ability to inhibit myostatin (10 ng/mL) or activin A (10 ng/mL)-induced Smad2/3 response in a CAGA-luciferase reporter gene assay in HEK293T/17 cells.

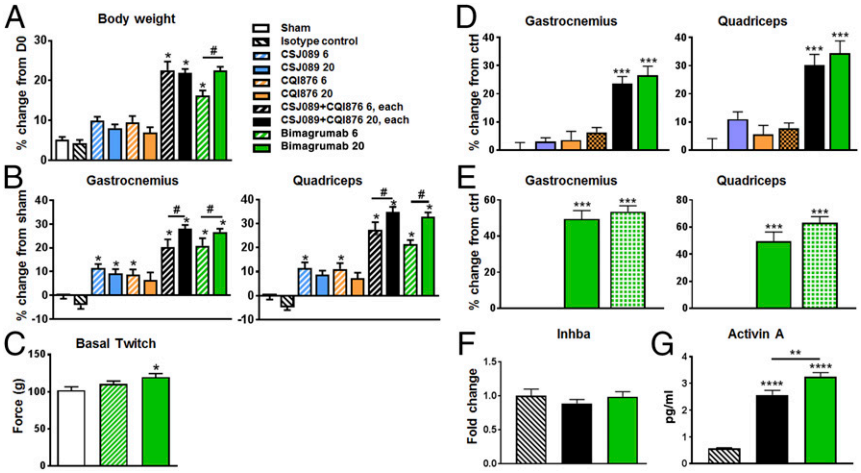

Fig. 4. Hypertrophy response as measured via (*A*) body weight, (*B*) muscle weight change from sham group, after 4-wk treatment with ActRIIA-specific Ab, ActRIIB-specific Ab, combination thereof, and bimagrumab in SCID mice ($n = 12$ per group). Mice were untreated, sham group (white), or treated with weekly s.c. injection of isotype control antibody (20 mg/kg/wk) or of anti-ActRIIA Ab (CSJ089, blue, 6 or 20 mg/kg), an anti-ActRIIB Ab (CQI876, orange, 6 or 20 mg/kg), a combination of CSJ089 and CQI876 (black, 6 or 20 mg/kg of each Ab), or bimagrumab (green, 6 or 20 mg/kg). (*C*) Invasive muscle contractile function determination in gastrocnemius muscle of sham (white) and bimagrumab (green, 6 and 20 mg/kg)-treated groups, average of three stimulations. Hypertrophy response was measured through gastrocnemius and quadriceps muscle weight changes in SCID mice, (*D*) after 2-wk treatment with the same antibodies as in *A*, all dosed at 20 mg/kg, with CQI876 being also dosed at 100 mg/kg (orange crosses), (*E*) after 4-wk treatment with weekly s.c. injection of isotype control antibody (stripes), dual anti-ActRIIA/ActRIIB Ab (CDD861, green pattern, 20 mg/kg), and bimagrumab (green, 20 mg/kg). (*F*) Activin A (inhba gene) expression changes in gastrocnemius muscle of SCID mice, after 2-wk treatment with isotype control, combination of anti-ActRIIA and anti-ActRIIB Abs (black), or bimagrumab (green) as in *D*. (*G*) ELISA data for activin A level in serum from mice of *D*/*F*. Data are presented as mean ± SEM analyzed using one-way ANOVA; differences vs. control were considered statistically significant, $*P < 0.05$; $**P < 0.01$; $***P < 0.001$; $****P < 0.0001$. Unpaired *t* test 20 vs. 6 mg/kg, $\#P < 0.05$.

for the two receptors, in comparison with bimagrumab yielded very similar responses in 4-wk studies (Fig. 4*F*). Additionally, the very same magnitude of response upon single versus dual receptor blockade was observed in a 4-wk rat study (*SI Appendix*, Fig. S5*C*). Upon complete receptor inhibition, either through a combination of anti-ActRIIA and anti-ActRIIB antibodies or by using the dual-receptor inhibiting bimagrumab treatments, increased circulating levels of activin A were detected (Fig. 4*G*). While this occurred, expression levels of activin A (Inhba gene) in skeletal muscle remained unchanged (Fig. 4*F*), as also reported in Latres et al. (18) upon use of ActRIIB-Fc for Inhba, pointing toward circulating ligand accumulation due to receptor blockade by the antibodies, preventing ligand internalization and subsequent degradation.

Muscle functional responses were monitored in the 6 or 20 mg/kg bimagrumab groups in SCID mice, treated for 4 wk, using an in situ evaluation of contractile function (Fig. 3*C*). An increase in basal isometric twitch force of the gastrocnemius muscle was observed, reaching significance only in the highest dose group of mice for which the muscle mass gain was the most important.

Discussion

Bimagrumab exhibits picomolar binding affinity toward both the ActRIIA and the ActRIIB LBD, which is surprising in view of the relatively low (55%) amino acid sequence identity between these two receptor subtypes. Our crystallographic studies demonstrate that bimagrumab binds the ActRIIA and ActRIIB LBD in essentially the same way and prevents signaling through these receptors by blocking their ligand binding surface on the LBD. The very high, single-digit picomolar binding affinity of bimagrumab toward the ActRIIB LBD results from an unusually good shape complementarity, combined with strong electrostatic and hydrophobic interactions involving all six CDRs, and a mainly lock-and-key-fit mechanism of association. The relatively weaker, but still subnanomolar binding to the ActRIIA LBD can be ascribed to two mutations affecting important epitope residues, which lead to a reduction in the size of the binding interface and in the total number of intermolecular interactions.

Activin A, GDF11, and myostatin have been reported to bind ActRIIA and ActRIIB albeit with different affinities (13, 37), in contrast to original findings highlighting binding of myostatin to ActRIIB (20). At a cellular level, and on cells expressing similar level of ActRIIA and ActRIIB, treatment with single-specificity antibody, either anti-ActRIIA or anti-ActRIIB, reduced Smad2/3 downstream signaling by 30–50% only, clearly demonstrating that myostatin and activin A engage both receptors for triggering of their cellular response, and that blockade of a single receptor does not preclude response via the remaining one. This observation was independent of antibody affinity and was confirmed with several other specific neutralizing antibodies (example provided in *SI Appendix*, Fig. S5). Only the combined use of the anti-ActRIIA and anti-ActRIIB antibodies or the use of dual antibodies bimagrumab and CDD861 allowed for complete blockade of the myostatin or activin A response. The full Smad2/3 signaling blockade achieved with bimagrumab was two- to threefold more potent than with the combined use of anti-ActRIIA and anti-ActRIIB Abs, possibly due to higher affinities of bimagrumab toward the two receptors, compared with the two specific antibodies used, or to dual specificity of a single antibody leading to unique engagement and blockade of ActRIIA and ActRIIB complexes. Indeed, both dual neutralizing antibodies bimagrumab and CDD861 exhibited lower IC_{50} of blocking myostatin or activin A signaling, despite slightly different affinities for ActRIIA and ActRIIB as well as different selectivity.

Whereas ActRIIA-specific and ActRIIB-specific antibodies showed moderate skeletal muscle hypertrophy when administered alone, their combination induced hypertrophy exceeding a simple additive effect of the two antibodies and similar to bimagrumab, confirming that the combination of anti-ActRIIA and anti-ActRIIB inhibition is superior to either single ActRIIA or ActRIIB inhibition. Indeed, the muscle mass increase achieved with bimagrumab is strikingly superior compared with the effect achieved by blocking either receptor alone, suggesting that functionally, at the

efficacious doses used, bimagrumab works by blocking both receptors. The apparent lack of a dose–response on body weight with either the anti-ActRIIA– or the anti-ActRIIB–specific antibodies suggested that target saturation was already achieved at 6 mg/kg, whereas the effect of the combination of both antibodies was additive. However, Lee et al. reported no gene dosage feature, i.e., no phenotype in heterozygous ActRIIA and ActRIIB mice (11), and hypertrophy only in full single knockout mice.

While multiple ligands, activin A, activin B, myostatin, GDF11, BMP9, and BMP10 have been reported to bind ActRIIs in various biochemical or cellular systems (13), some also signal via additional receptors, such as BMPRII. A newer generation of ligand trap of the TGF-β superfamily deprived of BMP9/10 binding has come forward (38) to alleviate some vascular findings likely related to BMP9/10 neutralization observed with the first generation of soluble ActRIIB decoy (27, 39). No such effects related to activating BMPs have been observed with bimagrumab so far (40–42). Aside for the myostatin/activin/Smad2/3 muscle inhibitory pathway, a key role of the BMP/Smad1/5 pathway at promoting muscle growth and regulating its maintenance has been reported simultaneously by two groups (43, 44). A strong interplay between inhibition of the muscle growth repressing Smad2/3 pathway and the converse activation of the growth promoting BMP/Smad1/5 axis has been identified (19, 43, 44). With the strong anabolic response ascribed to inhibition of ActRII/Smad2/3 observed upon bimagrumab administration, we cannot fully exclude a component coming from activation of the Smad1/5 axis, despite lack of evidence at this stage.

Blocking myostatin alone in adult mice induces around 15% hypertrophy (21, 22), much lower than the anabolic gain reported here with bimagrumab or combination of the two anti-ActRII antibodies, which illustrates that other ligands in addition to myostatin are contributing to the inhibition of skeletal muscle through these receptors—probably mostly activin A, based on blood levels (22). Evidence reported in elderly humans treated with anti-myostatin neutralizing antibody demonstrates a smaller magnitude of muscle mass changes, such as an appendicular lean body mass (aLBM) increase of 2–3% (23, 45), while studies conducted in sporadic inclusion body myositis and sarcopenia patients with bimagrumab demonstrated aLBM changes of 5–6% (41, 42).

Thus, to achieve strong therapeutic benefit in the treatment of muscle wasting conditions, myostatin inhibition and single activin type II receptor blockade are both less effective than dual receptor blockade with the single agent, bimagrumab. If one were to achieve this same effect with an antibody to the ligands, it would be necessary to simultaneously inhibit myostatin, activins, and perhaps GDF11 as well, in those conditions in which it is elevated (46).

Materials and Methods

Material and Reagents. All recombinant proteins were from R&D Systems and the hActRIIB$^{19\text{-}137}$-hFc fusion protein was produced internally. Monoclonal antibodies against ActRIIA (CSJ089 and CQI872) and ActRIIB (CQI876), or both receptors (CDD861), were identified utilizing human Fab phage display libraries (HuCAL, HuCAL PLATINUM; MorphoSys AG), selected for neutralization of myostatin binding to ActRIIA and ActRIIB. Anti-chicken lysozyme Ab (isotype control Ab), anti-ActRIIA (CSJ089 and CQI872), anti-ActRIIB (CQI876), bimagrumab, and CDD861 were all obtained from Novartis. "All data relevant to the article are available upon request without restriction. Materials disclosed herein may be made available upon request under a material transfer agreement." Secondary Ab, anti-human IgG (H+l) Alexa 647 was from Invitrogen.

Affinity Measurement Through Biacore. Surface plasmon resonance (SPR) measurements were performed using a Biacore T200 equipped with a protein A sensor chip (GE Healthcare). The human ActRIIA and ActRIIB-Fc proteins (R&D Systems) were captured at a density of ~100 resonance unit on the chip. Flow cell 1 served as a reference. The kinetic binding data were collected by subsequent injections of 1:2 dilution series of the Fabs (ranging from 0.2 to 50 nM). The surfaces were regenerated with 10 mM glycine-HCl, pH 1.5. The raw data were double referenced, i.e., response of the measuring flow cell was corrected for response of the reference flow cell, and in a second step, response of a blank injection was subtracted. The sensorgrams were fitted by applying a 1:1 binding model (global Rmax and local RI) to calculate kinetic rate and dissociation equilibrium constants. Three independent assays were performed.

Cell Culture. HEK293T/17 cells (ATCC) were stably transfected with a (CAGA) 12-luciferase reporter gene derived from the PAI-1 promoter cloned into pGL3 reporter construct (Promega) and cultivated in DMEM (4.5 g/L high glucose, w/o L-glutamine, w/o sodium pyruvate) supplemented with 10% FCS (Gibco), 1% glutamine (Invitrogen), pen/strep 1× (Invitrogen), 1 mM sodium pyruvate (Sigma), 5 μg/mL blasticidin (Gibco).

Flow Cytometry Analysis. HEK293T/17 cells were stained with anti-ActRII as well as isotype control antibodies, and an Alexa Fluor 647-conjugated goat anti-human IgG secondary antibody. Just before FACS analysis on a FACSCalibur instrument, 20 μL of To-Pro solution (Invitrogen) was added and acquisition performed using FL-1 (dead cell) and FL-4 (Alexa 647) using Cellquest Pro software. Fluorescent intensity (FL-4) of bound anti-ActRII antibodies was plotted and the mean fluorescence intensity (MFI) derived.

Reporter Gene Assay. Stable CAGA12-Luc transfected HEK293T/17 cells were stimulated and the reporter gene activity was measured using Britelite Plus (Perkin-Elmer), on a spectrophotometer (Spectramax M5; Molecular Devices).

Animal Efficacy Studies. Animal experiments were performed according to Swiss animal welfare standards on animal experimentation after approval by cantonal veterinarian authorities under license number BS-2476. The following efficacy studies were performed: (*i*) Dose–response efficacy of the anti-ActRIIA Ab, anti-ActRIIB Ab, and bimagrumab in naive SCID mice for 4 wk. Twelve-week-old male CB-17 SCID mice (Janvier Laboratories) were randomized based on body weight and untreated or treated with weekly s.c. injections of vehicle (isotype control), anti-ActRIIA Ab (CSJ089), anti-ActRIIB Ab (CQI876), a combination of both CSJ089 and CQI876, or bimagrumab, at 6 or 20 mg/kg/wk for 4 wk, the mice receiving the combination treatment, administered 6 or 20 mg/kg of each Ab, i.e., a total dose of 12 and 40 mg/kg. Body weight was monitored weekly and on day 28, mice were anesthetized to evaluate their muscle strength (detailed procedure below). Mice were killed with CO_2, serum, and the gastrocnemius with plantaris muscle, quadriceps muscle, tibialis anterior muscle, soleus muscle, and the extensor digitorum longus (EDL) muscle were collected and weighed as well as various organs (heart, liver, white adipose tissue, kidney, and testis). The tibialis muscle was embedded in OCT and frozen in liquid nitrogen-cooled isopentane and processed for histological analysis. (*ii*) Efficacy study of the anti-ActRIIA Ab, anti-ActRIIB Ab, CDD861, bimagrumab in naive SCID male mice for 2 wk. Twelve-week-old mice were treated weekly s.c. with isotype control, anti-ActRIIA Ab (CSJ089), anti-ActRIIB Ab (CQI876), combination of both CSJ089 and CQI876, dual ActRIIA/ActRIIB Ab (CDD861), or bimagrumab, all at 20 mg/kg, with an additional group of CQI876 also at 100 mg/kg. Body weight was recorded once weekly and the mice were killed as specified above. The gastrocnemius muscle and tibialis anterior muscle were harvested and weighed. (*iii*) Profiling of anti-ActRIIA Ab, anti-ActRIIB Ab, and bimagrumab in naive rats for 4 wk. A total of 20 mg/kg of isotype control, CSJ089, CQI876, or a combination of both Abs, were injected weekly i.v. in 12-wk-old Wistar rats. After 28 d, rats were killed and the tibialis anterior muscle, quadriceps muscle, and gastrocnemius muscle were dissected and weighed.

In Situ Evaluation of Contractile Function. In mice deeply anesthetized with isoflurane, the distal tendon of the gastrocnemius muscle was attached to a force transducer (Grass Technologies). The muscle was stimulated through an electrode (Hugo Sachs Electronik) on the sciatic nerve adjusted to reach an optimum length for the development of isometric twitch force. An electric stimulation was preceded with a single electrical pulse to produce a twitch response. The voltage of stimulation was adjusted to produce a maximal twitch response. Muscle was rested for 20 s between twitch responses. Optimal muscle length was achieved when twitch force was maximal. The muscle was stimulated at increasing frequencies from 10 to 160 Hz, with stimulation for 300 ms and rest for 30 s between successive stimuli. The frequency force relationship was derived afterward. Maximum absolute isometric tetanic force was determined from the plateau of the frequency–force relationship.

Statistical Analysis. All results are presented as mean ± SEM and were analyzed using one- or two-way analysis of variance (ANOVA), differences after Bonferroni post hoc test were considered statistically significant or unpaired

two-tailed Student *t* test according to the experimental design. Values were considered statistically significant at $*P < 0.05$; $**P < 0.01$.

Purification and Crystallization of the Bimagrumab Fab. The bimagrumab Fab was expressed in *Escherichia coli* TG1^{-}, purified by metal chelation and cation exchange chromatography and concentrated by ultrafiltration to 9.8 mg/mL in 10 mM Tris, pH 7.4, 25 mM NaCl. Fab crystals grew from 18% PEG 5,000 monomethylether, 50 mM Tris pH 8.0.

Expression and Purification of the ActRIIA LBD. The ActRIIA LBD (Uniprot entry P27037, amino acid residues 20–134) with an APP-tag (EFRHDS) was expressed in HEK293-6E cells and purified by anti-tag affinity chromatography followed by size-exclusion chromatography.

Expression and Purification of the ActRIIB LBD. The ActRIIB LBD (Uniprot entry Q13705, amino acid residues 24–117) was cloned as a cleavable thioredoxin-His6 fusion protein, expressed intracellularly in *E. coli* Shuffle and purified by metal chelation chromatography.

Purification and Crystallization of the ActRIIB LBD Fv Complex. The Bimagrumab Fv was expressed in *E. coli* W3110, purified by metal chelation and size-exclusion chromatography and mixed with 1.4-fold molar excess of the thioredoxin-His_6 fusion protein. Cleavage of the thioredoxin fusion was performed on the protein complex using PreScission protease. The Fv complex was then purified by anion exchange and size-exclusion chromatography and concentrated to 6–10 mg/mL for crystallization screening. Cubic crystals diffracting to 3.35 Å were obtained from 1.4 M ammonium sulfate, 0.1 M sodium acetate, pH 4.6. Orthorhombic crystals diffracting to high resolution grew after 2 mo from 0.1 M phosphate-citrate buffer pH 5.4, 40% PEG 300.

Purification and Crystallization of the ActRIIA LBD Fv Complex. The bimagrumab Fv and the ActRIIA LBD were mixed at a 1:1 molar ratio and the complex was purified by size-exclusion chromatography, concentrated to 12.6 mg/mL and crystallized. Monoclinic crystals grew from 0.1 M sodium citrate tribasic, 25% wt/vol PEG 3350.

Crystallographic Data Collection, Structure Determination, and Refinement. All diffraction data were collected at the Swiss Light Source, beamlines PX-II and PX-III. Structures were solved by molecular replacement and refined using standard crystallographic methods.

ACKNOWLEDGMENTS. We thank Stefan Dalcher and Andrea Gerber for the cloning, expression, and purification of the human ActRIIA LBD; Martin Geiser, Julia Klopp, and Sébastien Rieffel for the cloning, expression, and purification of the human ActRIIB LBD; Karen Vincent, Claudia Corinna Henke, Matthias Ryszka, Frank Hillger, Laurent Weiss, and Sabrina Seddik for the cloning, expression, and purification of the bimagrumab Fab and Fv fragments; Mauro Zurini for the purification of antigens and antibodies used throughout; and Sandra Walter for some SPR work. We are grateful to the machine and beamline groups of the Swiss Light Source, Paul Scherrer Institute, Villigen, Switzerland and the Muscle Diseases group at the Novartis Institutes for Biomedical Research (NIBR) for their enthusiastic support, along with the rest of the NIBR community, in particular Novartis Biologics Center and Chemical Biology and Therapeutics groups for their support.

1. Egerman MA, Glass DJ (2014) Signaling pathways controlling skeletal muscle mass. *Crit Rev Biochem Mol Biol* 49:59–68.
2. Bodine SC (2013) Disuse-induced muscle wasting. *Int J Biochem Cell Biol* 45: 2200–2208.
3. Glass D, Roubenoff R (2010) Recent advances in the biology and therapy of muscle wasting. *Ann N Y Acad Sci* 1211:25–36.
4. Morley JE (2012) Sarcopenia in the elderly. *Fam Pract* 29:i44–i48.
5. Han HQ, Zhou X, Mitch WE, Goldberg AL (2013) Myostatin/activin pathway antagonism: Molecular basis and therapeutic potential. *Int J Biochem Cell Biol* 45:2333–2347.
6. Zimmers TA, et al. (2002) Induction of cachexia in mice by systemically administered myostatin. *Science* 296:1486–1488.
7. McPherron AC, Lawler AM, Lee SJ (1997) Regulation of skeletal muscle mass in mice by a new TGF-beta superfamily member. *Nature* 387:83–90.
8. McPherron AC, Lee SJ (1997) Double muscling in cattle due to mutations in the myostatin gene. *Proc Natl Acad Sci USA* 94:12457–12461.
9. Schuelke M, et al. (2004) Myostatin mutation associated with gross muscle hypertrophy in a child. *N Engl J Med* 350:2682–2688.
10. Lee SJ, et al. (2010) Regulation of muscle mass by follistatin and activins. *Mol Endocrinol* 24:1998–2008.
11. Lee SJ, et al. (2005) Regulation of muscle growth by multiple ligands signaling through activin type II receptors. *Proc Natl Acad Sci USA* 102:18117–18122.
12. Trendelenburg AU, Meyer A, Jacobi C, Feige JN, Glass DJ (2012) TAK-1/p38/nNFκB signaling inhibits myoblast differentiation by increasing levels of activin A. *Skelet Muscle* 2:3.
13. Souza TA, et al. (2008) Proteomic identification and functional validation of activins and bone morphogenetic protein 11 as candidate novel muscle mass regulators. *Mol Endocrinol* 22:2689–2702.
14. McPherron AC, Huynh TV, Lee SJ (2009) Redundancy of myostatin and growth/differentiation factor 11 function. *BMC Dev Biol* 9:24.
15. Sinha M, et al. (2014) Restoring systemic GDF11 levels reverses age-related dysfunction in mouse skeletal muscle. *Science* 344:649–652.
16. Egerman MA, et al. (2015) GDF11 increases with age and inhibits skeletal muscle regeneration. *Cell Metab* 22:164–174.
17. Hinken AC, et al. (2016) Lack of evidence for GDF11 as a rejuvenator of aged skeletal muscle satellite cells. *Aging Cell* 15:582–584.
18. Latres E, et al. (2017) Activin A more prominently regulates muscle mass in primates than does GDF8. *Nat Commun* 8:15153.
19. Chen JL, et al. (2017) Specific targeting of TGF-β family ligands demonstrates distinct roles in the regulation of muscle mass in health and disease. *Proc Natl Acad Sci USA* 114:E5266–E5275.
20. Rebbapragada A, Benchabane H, Wrana JL, Celeste AJ, Attisano L (2003) Myostatin signals through a transforming growth factor beta-like signaling pathway to block adipogenesis. *Mol Cell Biol* 23:7230–7242.
21. Whittemore LA, et al. (2003) Inhibition of myostatin in adult mice increases skeletal muscle mass and strength. *Biochem Biophys Res Commun* 300:965–971.
22. Latres E, et al. (2015) Myostatin blockade with a fully human monoclonal antibody induces muscle hypertrophy and reverses muscle atrophy in young and aged mice. *Skelet Muscle* 5:34.
23. Becker C, et al.; STEADY Group (2015) Myostatin antibody (LY2495655) in older weak fallers: A proof-of-concept, randomised, phase 2 trial. *Lancet Diabetes Endocrinol* 3: 948–957.
24. Bogdanovich S, Perkins KJ, Krag TOB, Whittemore LA, Khurana TS (2005) Myostatin propeptide-mediated amelioration of dystrophic pathophysiology. *FASEB J* 19: 543–549.
25. Goncalves MD, et al. (2010) Akt deficiency attenuates muscle size and function but not the response to ActRIIB inhibition. *PLoS One* 5:e12707.
26. Zhou X, et al. (2010) Reversal of cancer cachexia and muscle wasting by ActRIIB antagonism leads to prolonged survival. *Cell* 142:531–543.
27. Attie KM, et al. (2013) A single ascending-dose study of muscle regulator ACE-031 in healthy volunteers. *Muscle Nerve* 47:416–423.
28. Lach-Trifilieff E, et al. (2014) An antibody blocking activin type II receptors induces strong skeletal muscle hypertrophy and protects from atrophy. *Mol Cell Biol* 34: 606–618.
29. Hatakeyama S, et al. (2016) ActRII blockade protects mice from cancer cachexia and prolongs survival in the presence of anti-cancer treatments. *Skelet Muscle* 6:26.
30. Chen Y, et al. (2014) Regulation and actions of activin A and follistatin in myocardial ischaemia-reperfusion injury. *Cytokine* 69:255–262.
31. Greenwald J, Fischer WH, Vale WW, Choe S (1999) Three-finger toxin fold for the extracellular ligand-binding domain of the type II activin receptor serine kinase. *Nat Struct Biol* 6:18–22.
32. Allendorph GP, Vale WW, Choe S (2006) Structure of the ternary signaling complex of a TGF-beta superfamily member. *Proc Natl Acad Sci USA* 103:7643–7648.
33. Greenwald J, et al. (2003) The BMP7/ActRII extracellular domain complex provides new insights into the cooperative nature of receptor assembly. *Mol Cell* 11:605–617.
34. Weber D, et al. (2007) A silent H-bond can be mutationally activated for high-affinity interaction of BMP-2 and activin type IIB receptor. *BMC Struct Biol* 7:6.
35. Greenwald J, et al. (2004) A flexible activin explains the membrane-dependent cooperative assembly of TGF-beta family receptors. *Mol Cell* 15:485–489.
36. Thompson TB, Woodruff TK, Jardetzky TS (2003) Structures of an ActRIIB:activin A complex reveal a novel binding mode for TGF-beta ligand:receptor interactions. *EMBO J* 22:1555–1566.
37. Walker RG, et al. (2017) Structural basis for potency differences between GDF8 and GDF11. *BMC Biol* 15:19.
38. Mulivor A, et al. (2014) G.P.205. *Neuromuscular Disord* 24:878.
39. Campbell C, et al. (2017) Myostatin inhibitor ACE-031 treatment of ambulatory boys with Duchenne muscular dystrophy: Results of a randomized, placebo-controlled clinical trial. *Muscle Nerve* 55:458–464.
40. Garito T, et al. (2017) Bimagrumab improves body composition and insulin sensitivity in insulin-resistant individuals. *Diabetes Obes Metab*, 10.1111/dom.13042.
41. Rooks D, et al. (2017) Treatment of sarcopenia with bimagrumab: Results from a phase II, randomized, controlled, proof-of-concept study. *J Am Geriatr Soc* 65: 1988–1995.
42. Amato AA, et al. (2014) Treatment of sporadic inclusion body myositis with bimagrumab. *Neurology* 83:2239–2246.
43. Winbanks CE, et al. (2013) The bone morphogenetic protein axis is a positive regulator of skeletal muscle mass. *J Cell Biol* 203:345–357.
44. Sartori R, et al. (2013) BMP signaling controls muscle mass. *Nat Genet* 45:1309–1318.
45. Woodhouse L, et al.; STUDY INVESTIGATORS (2016) A phase 2 randomized study investigating the efficacy and safety of myostatin antibody LY2495655 versus placebo in patients undergoing elective total hip arthroplasty. *J Frailty Aging* 5:62–70.
46. Schafer MJ, et al. (2016) Quantification of GDF11 and myostatin in human aging and cardiovascular disease. *Cell Metab* 23:1207–1215.